Power plant boilers operate at relatively high temperatures and pressures. As they are prone to material degradation, fouling and scaling, the materials used must have good thermal and chemical resistance. Coating material is one of the solutions to problems that exist in boilers. In this study, the basic coating material used came from local mineral resources, namely Kalimantan zircon sand and zirconia that had been purified from zircon sand. And there is the addition of filler as a coating reinforcement so that the coating properties become better. The variables of this study are variations of filler materials that have lubricating properties such as hBN, MoS$_2$, graphite and a mixture of the three fillers (hybrid). The coating method used is slurry spray coating and then sintering at 600 °C. The main coating parameter tests carried out were thermal shock and anti-fouling resistance. From the research results, it was found that the purification of zircon sand resulted in an increase in Zirconia content from 59 % to 68 %. From the results of the thermal shock resistance and anti-fouling tests, it was found that the coating with purified zircon has better thermal shock resistance while the fouling resistance is not significantly different from unrefined zircon sand, so it is necessary to develop a zircon purification process to obtain a higher ZrO$_2$ content. For filler variations, the hybrid filler produces a coating with better thermal shock and anti-fouling resistance so that it can be used for optimizing ceramic composite coatings

Keywords: zircon sand ceramic coating, purified zircon ceramic coating, lubricant, slurry spray, thermal shock, fouling resistance

ANALYSIS OF THE THERMAL SHOCK AND FOULING RESISTANCE OF THE KALIMANTAN ZIRCON BASED HYBRID COMPOSITE CERAMIC COATING IN BOILER ENVIRONMENT

Yulinda Lestari
Master of Engineering*

Anne Zulfia
Corresponding author
Doctor of Engineering, Professor
Department of Metallurgy and Materials Engineering
University of Indonesia
Kampus Baru UI Depok, Jawa Barat, Indonesia, 16424
E-mail: anne@metal.ui.ac.id

Muhammad Ardin
Bachelor of Engineering**

Septian Adi Chandra
Bachelor of Engineering*

Fauzi Widyawati
Bachelor of Science**

Efendi Mabruri
Doctor of Engineering, Professor*
*Research Center for Metallurgy
National Research and Innovation Agency (BRIN)
Puspiptek Serpong area, 470, Tangerang Selatan, Indonesia, 15314
**Department of Metallurgy Engineering
Sumbawa Engineering University
Batu Alang, Moyo Hulu, Sumbawa Besar, Indonesia, 84371

1. Introduction

The common problems in boilers are fouling and slagging. Slagging and fouling are very serious because they can have a major impact on boiler operations, such as heat transfer problems, decreased boiler efficiency, pipe blockages, and pipe damage due to clinker release. This problem will shorten the life of the boiler as well as other components in the power plant, resulting in economic losses. To overcome these problems, many methods have been applied such as selection of creep and corrosion-resistant materials [1], modification of material composition [2], modification of process flow, manipulation of process conditions [3], and modification of surface heat transfer to remove fouling and clean it [4]. The latest solution being developed is the modification of the pipe surface by adding an anti-fouling coating to reduce the adhesion of fouling and other contaminants that are deposited [5, 6]. This modification process is an interaction between the metal surface and the mechanism of the contaminants that are deposited such as attachment, adhesion, retention and then release from the pipe wall. This interaction indicates the adhesion strength of an anti-fouling coating and the ability to clean a surface.

The development of material coatings was driven by the need to overcome the limitations of traditional coatings,

such as limited adhesion, poor wear resistance and low corrosion resistance. Composite coatings offer a solution to this limitation by combining the desired properties of several different materials, such as their resistance to extreme conditions, hardness, toughness, and chemical resistance, into a single layer. This composite coating material was chosen based on ceramic materials because ceramic coatings have been widely used to improve metal properties by increasing refractory properties, insulation, erosion resistance, oxidation and corrosion resistance, heat resistance, electrical resistance, or improving optical properties. Ceramic coatings are needed in the industrial world for various applications, therefore the requirements and specifications for coatings also vary according to the application [6].

2. Literature review and problem statement

The paper [7] used a combination of SiO_2, Al_2O_3 and ZrO_2 as a ceramic coating with copper substrate using the slurry method. From the results of the study in terms of bonding, friction, wear, microstructure and thermal shock test parameters, it is shown that the ceramic coating increases the resistance of copper at high temperatures. While the paper [8] examined a ceramic coating from zircon ground powder with a composition of 63.00 ZrO_2, 32.50 SiO_2, <2.00 Al_2O_3, <1.30 HfO_2, <0.15 TiO_2, 0.07 Fe_2O_3 and 1.00 LOI (in oxide wt %) using the suspension plasma spraying method. With two zircon suspension feedstocks (10 and 30 vol %) variation, it is shown that SPS improves the adherence of the coating to the substrate, and an increase in the solids content from 10 vol % to 30 vol % leads to a higher amount of zirconia, lower amorphous phase and lower t/m ratio (higher monoclinic phase). From the papers [7] and [8], which use a zircon matrix with finer particle sizes, it produces better physical and thermal shock properties. So it is necessary to purify and refine zircon sand grains before being used as a coating matrix. There has been no specific research on the use of Kalimantan zircon sand for coating materials. But there are some challenges that must be faced, such as the content of other oxides in the Kalimantan zircon sand, which will affect the resulting coating compared to using pure zirconia.

There are various lubricants that function as fillers in coatings to increase their thermal and fouling resistance, such as h-BN, SiC, CNT, MoS_2, WS_2, and graphite [9]. The filler has a function to enhance certain properties of the coating, such as to enhance the adhesive strength, increase cracking resistance, erosion resistance, heat resistance, and so on. The effect is given by the filler depending on the size and shape of the particles (isometric, cubic, hexagonal, laminar) [10]. The use of hexagonal boron nitride is familiar in ceramic composite coating. The paper [11] classified this hBN as a lubrication material that is resistant to extreme temperatures. The paper [12] made a review of hBN regarding its preparation and application in composite coatings. The excellent mechanical properties of hBN make this BN have good ceramic machinability. Its thermal properties are also stable under extreme conditions and have superhydrophobic properties. Hexagonal boron nitride (h-BN) has a lamellar structure and bonds covalent on strong B-N. h-BN is a material that has a high temperature resistance, oxidation resistance, high thermal conductivity, and good corrosion resistance against alkalis, acids, and glass-like slags [13].

In the paper [14], MoS_2 and graphite were used as fillers in the YSZ Thermal barrier coating. From the morphological and mechanical results of the coating, it is shown that the presence of MoS_2 and graphite can increase the cohesive strength of the YSZ coating. The research in papers [15, 16] showed that MoS_2 and graphite can function as lubricant materials in ceramic coatings and provide improvements in the mechanical properties and corrosivity of coatings. MoS_2 is a transition metal material that has unique properties such as symmetrical and hexagonal crystal forms [17]. MoS_2 can also be used as a passive filler and lubricant then has a low coefficient of friction and good thermal stability in non-oxidizing and high-temperature environments.

Graphite is one of the polymorphs of carbon, which has the same structure and consists of hexagonally arranged layers of carbon atoms. Graphite has a density characteristic of 2.26 g/cm^3 [18]. In each layer, each carbon atom bonds to 3 coplanar with other atoms through strong covalent bonds. Fourth electron bonds are bonded between layers by weak Van der Waals bonds. So due to weak interplanar bonds, bond-breaking interplanar is made easy. This makes graphite have the properties of good lubrication and high electrical conductivity. Graphite has high strength properties, chemical stability at high temperatures and a good nonoxidizing atmosphere, high thermal conductivity, low coefficient of thermal expansion and good thermal shock resistance [19]. Therefore, the three filler materials, such as hBN, MoS_2 and graphite, will be compared and combined (hybrid) so that it is expected to increase the resistance of the coating at high temperature conditions.

Ceramic coating using the slurry method is widely used because it is easier to apply, resulting in a coating with good properties and being more economical. Coatings with the slurry method produce good bonding, thermal shock, thermal oxidation, hardness, and corrosivity resistance [7, 20, 21].

Thermal shock and anti-fouling testing of ceramic coatings is essential to see the durability and toughness of coatings in extreme environments. In [22], a ceramic coating for the TiO_2 substrate was made with the Plasma Electrolytic Oxidation method. With the addition of nano-ZrO_2, it is proven to be able to increase its thermal shock resistance. The paper [23] conducted thermal shock testing for the Thermal Barrier Coating with several layers of coating. After the thermal shock process on the coating, a reduction in coating thickness occurred, and some samples suffered cracks and damage. Likewise, the results of research in [24] for thermal shock testing on the Thermal Barrier coating with several layers with variable heat treatment also showed degradation on the material surface during the thermal shock process. Important aspects of surface coatings are durability, stability and cost effectiveness under conditions of repeated operation (fouling and cleaning). The paper [25] demonstrated coating performance during repeated fouling and cleaning processes and concluded that when a coating loses its bond, this is an indication that a material's service life will expire. This fouling causes an increase in pressure drop and a decrease in heat transfer. The thermal impact of fouling is described as fouling resistance (Rf), which is related to deposit thickness (δf), and thermal conductivity (λf). This fouling resistance can be expressed by the formula:

$$Rf = \frac{\delta f}{\lambda f}. \qquad (1)$$

As the deposit layer increases, the Rf value increases and the temperature at the interface of the process stream and deposit changes. This affects the rate of deposit formation [26].

So from the results of these studies, it can be said that this test method is very suitable to be used to see the performance and resistance of coatings at high temperatures. All of this allows us to emphasize that it is necessary to conduct research on zirconia-based ceramic coating composites from local minerals that have thermal shock and fouling resistance in high-temperature applications.

3. The aim and objective of this study

The aim of the study is to identify the thermal shock and fouling resistance of the Kalimantan zircon based hybrid composite ceramic coating. This will make it possible to improve the durability of ceramic coatings on degradation material in high-temperature applications.

To achieve this aim, the following objectives are accomplished:

– to purify Kalimantan zircon sand to obtain higher zirconia content;

– to analyze the coating's thermal shock resistance;

– to analyze the coating's anti-fouling resistance.

4. Materials and method of the research

4. 1. Object and hypothesis of the study

The choice of anti-fouling coating material is related to the mechanism by which thermal conductivity is inversely proportional to fouling resistance. If high fouling resistance is desired, the thermal conductivity of the material is chosen that is not too high but sufficient to conduct heat. Based on this, a coating material based on zirconia ceramic composite was chosen.

The main raw material for coatings in this study came from local mineral materials, namely Kalimantan Zircon Sand. Besides utilizing abundant local resources in Kalimantan, Zircon Sand also contains lubricants that are anti-fouling, high temperature resistant and have good chemical stability. The material used for the coating mixture is Zirconia, which has been purified from Kalimantan zircon sand. Zirconia is too easily stabilized by other metal oxides to modify physical properties, mechanics, and chemistry. The low thermal expansion of zircon $(6.39{\times}10^{-6}$ cm/cm°C) exhibits high thermal shock resistance and resistance to spalling. Spalling is the deformation of a material due to an increased temperature [27]. There has been no specific research on the use of Kalimantan zircon sand for coating materials, making this research original. However, several studies on zirconia coatings rarely use composite coatings with additional fillers. So, this study will show the phenomenon of the coating surface with the addition of filler, whether it improves the microstructure.

The variable of this research is the type of filler, which functions as a lubricant for anti-fouling such as h-BN, MoS_2 and graphite. In the literature study, it has been explained that the best and most chemically and thermally stable material is h-BN, so the best fouling resistance results are possible with the h-BN filler. However, h-BN is quite expensive, especially if it is used a lot to coat boilers. Therefore, this alternative lubricant will be observed physically, mechan-
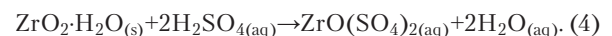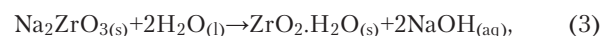
ically and which microstructure is closest to the results of h-BN lubricant.
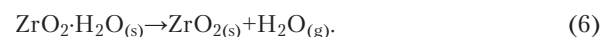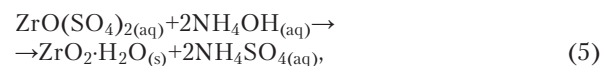
4. 2. Purification of Kalimantan zircon sand

Zircon oxide purification uses the wet milling process method, which produces quite high purity with a simpler process [28]. The purification of zirconia from zircon sand is preceded by the process of separation between ZrO_2 and SiO_2 bonds. The easiest method for separating the bonds of the two oxides is the fusion process [29]. The fusion process is a decomposition process using alkali metals, both sodium hydroxide (NaOH) and potassium hydroxide (KOH) as a reactor. Alkali metals (NaOH, KOH) function to decompose zircon at a certain temperature to form zirconate compounds, such as sodium zirconate, and sodium silicate [30]. The reaction that occurred during the fusion process is as in (2):

$$ZrSiO_4 + 4\ NaOH \rightarrow Na_2ZrO_3 + Na_2SiO_3 + 2\ H_2O\uparrow. \qquad (2)$$
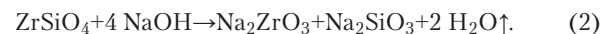
The next process is metal removal from the rock with the help of reagents, concentration of the resulting solution scraping, and purification, recovery is the removal of metal from solution scraping results. Erosion is a selective dissolution process, only metals are soluble. Solvents are liquids that from an engineering point of view must be cheap, capable of regeneration, and capable of dissolving the desired minerals quickly so that they can separate the minerals from the gangue material (impurities) [31]. The solvent will dissolve some of the solid material so that the material desired solute can be obtained. The selection of the washing method (leaching) depends on the valuable metal content in the ore and the characteristics of the ore especially whether or not the ore is easily washed by certain chemical reagents. One of the solvents that are often used is sulfuric acid (H_2SO_4). At room temperature, sulfuric acid is colorless and miscible with water [32]. Sulfuric acid reacts with all metals and has a boiling point of 340. Sulfuric acid is highly corrosive and has reactive hydration with highly exothermic water. The corrosive nature of sulfuric acid can damage metal objects. The reaction that occurred during the leaching process is as in (3) and (4):

$$Na_2ZrO_3{}_{(s)} + 2H_2O_{(l)} \rightarrow ZrO_2.H_2O_{(s)} + 2NaOH_{(aq)}, \qquad (3)$$

$$ZrO_2{\cdot}H_2O_{(s)} + 2H_2SO_4{}_{(aq)} \rightarrow ZrO(SO_4)_2{}_{(aq)} + 2H_2O_{(aq)}. \ (4)$$

The next process is precipitation and calcination, which is described in the following reaction:

$$ZrO(SO_4)_2{}_{(aq)} + 2NH_4OH_{(aq)} \rightarrow$$
$$\rightarrow ZrO_2{\cdot}H_2O_{(s)} + 2NH_4SO_4{}_{(aq)}, \qquad (5)$$

$$ZrO_2{\cdot}H_2O_{(s)} \rightarrow ZrO_2{}_{(s)} + H_2O_{(g)}. \qquad (6)$$

Zircon before and after being purified was analyzed for its chemical composition using an XRF benchstop PANalytical Epsilon 1 type. XRF is a tool used to analyze chemical composition and the concentration of elements contained in a sample using X-rays. XRF is generally used to analyze elements in minerals or rocks. Elemental analysis was carried out both qualitatively and quantitatively.

4. 3. Ceramic Coating Process

The coating process uses the slurry spray method. The slurry is made with variations in the type and composition

of the filler listed in Table 1 [6]. In this study, several fillers were selected, namely hBN, MoS_2 and graphite. Inorganic lubricants such as graphite, hBN, MoS_2 consist of a combination of tightly packed layers, in which the atoms are tightly bound to each other. However, the bonds between the two layers are not strong enough (e.g. van der Waals bonds). The crystalline layers of the lubricant are arranged in parallel, which decompose due to the relative speed of the dry sliding operation, and provide excellent anti-friction properties to the counter surface. However, sometimes this crystal structure alone is not enough to achieve tribological properties at high temperatures, it is necessary to combine several lubricants to improve the properties [33]. Therefore, a hybrid filler is used, which is a mixture of the three fillers. The first stage of slurry composites coating is the mixing process, where mixing is a process of mixing filler (Zirconia, BN, MoS_2, and graphite) and adding solvent material (aquadest), binder material (waterglass), and additives (sodium lauryl sulfate) in the coating process. Waterglass is a transparent film layer that has a three-dimensional structure and good water resistance, and can form strong bonds with steel substrates. Potassium silicate (waterglass) is an environmentally friendly binder and can form Si-O-Si bonds when the temperature exceeds 200 °C. Meanwhile, Sodium Lauryl Sulfate in this coating mixture functions as a dispersant, which prevents clumps of powder granules so that the coating mixture is more homogeneous. The mixing process was carried out with a magnetic stirrer for 60 minutes so that it is evenly mixed, then ultrasonic milling is carried out on the mixture for 60 minutes as a deagglomeration process [34]. The mixture was further processed with an ultrasonic bath for 1 hour [35]. After the mixing stage, the spraying process is carried out using a spray gun with compressor pressure adjusted to the surface of the sample by a distance between the sample and the spray gun of 10 cm and a time of 10 seconds.

Table 1

Composition of ceramic slurry coating

Materials	Sample Coating Name (wt %)							
	ZS1	ZS2	ZS3	ZS4	ZP1	ZP2	ZP3	ZP4
Zircon Sand	6	6	6	6	–	–	–	–
Purified Zircon	–	–	–	–	6	6	6	6
hBN Powder	3	–	–	1	3	–	–	1
MoS_2 Powder	–	3	–	1	–	3	–	1
Graphite Powder	–	–	3	1	–	–	3	1
Waterglass	18	18	18	18	18	18	18	18
Sodium Lauryl Sulfate (SLS)	5	5	5	5	5	5	5	5
Aquadest	68	68	68	68	68	68	68	68

After that, dried in a closed room so as not exposed to dust, then dried using an oven with a temperature of 110 °C for 1 hour, and stages were finally sintered at 600 °C for 6 hours coating (film layer) and adheres thoroughly to the surface of the sample (steel substrate). The coating sample is then ready for the next process, namely testing for thermal shock and anti-fouling resistance.

4. 4. Thermal Shock and Fouling Resistance Test

Thermal shock testing is carried out on each coating specimen that has been sintered. The coating material was heated at 600 °C for 10 minutes, then immediately immersed in water (room temperature) for 5 minutes and dried at room temperature. Specimens were observed for damage morphology using SEM-EDS [6]. The scanning electron microscope (SEM) produces an image of the surface of the test object by scanning the surface using a focused electron beam. The electrons interact with atoms on the surface, producing various signals that contain information about topgrade and composition. The SEM-EDS used for measurement is the JEOL type. From the microstructure of the coating surface, it is possible to measure the thermal shock resistance from the adhesion of the coating where delamination of more than 1/3 of the surface area of the coating has poor thermal shock resistance. This is also supported by the EDS data, which contains most Fe substrate elements [6].

The anti-fouling resistance test was carried out by applying fly ash powder to the coating surface. In this study, fly ash was replaced with sodium sulfate powder, which is the main component of fly ash. Sodium sulfate powder is polished on the surface of the coating, then dried in an oven at 100 °C for 1 hour. Coating specimens that had been polished with sodium sulfate were then heated in a muffle furnace at 600 °C for 24 hours and cooled at room temperature. After that, the morphology was observed using SEM-EDS [6]. The coating is expected to have hydrophobic properties to prevent contaminant contact with the substrate. Therefore, the coating must have a low percentage of porosity. Porosity makes the coating hydrophilic or water-absorbing. The percentage level and characteristic of coating porosity were analyzed using ImageJ Software. ImageJ has a Java plugin, which is used to solve many problems of image processing and image analysis up to three dimensions [36]. In this study, the percentage of porosity and profile stacks on the surface microstructure of the zircon ceramic composite layer with various fillers was measured in the conditions after the fouling resistance test.

5. Research results of thermal shock and fouling resistance of the Kalimantan zircon based hybrid composite ceramic coating

5. 1. Analysis of zirconia content in refined zircon

To find out the composition of the oxide produced from the refining of Kalimantan Zircon Sand, the XRF test is performed. A comparison of the composition of Kalimantan Zircon Sand and refined Zirconia is shown in Table 2. The purification of zircon sand aims to increase the Zirconia content so that the Zirconia properties in the coating mixture can be more dominant and increase its resistance.

The research results showed that the Zirconia content in the refined Kalimantan Zircon Sand increased after the refining process and reached 68 wt % ZrO_2.

Table 2

XRF test of zircon sand and purified zircon

Materials	Oxide Content (wt %)								
	ZrO_2	SiO_2	HfO_2	TiO_2	Al_2O_3	Fe_2O_3	P_2O_5	MgO	Y_2O_3
Kalimantan Zircon Sand	59.2	29.8	1.3	1.1	1.4	0.1	5.9	0.3	0.4
Purified Zirconia	68	7.9	1.4	0.5	2.8	0.5	16.6	0.4	0.3

5. 2. Thermal shock resistance
5. 2. 1. Zircon sand based ceramic composite coating

Fig. 1, *a–d* shows the microstructure of zircon sand coating samples with various fillers used, which were given thermal shock treatment at 600 °C for 10 minutes and then quenched. Fig. 1, *a* represents the microstructure of the ZS1 thermal shock sample in which the zircon sand is combined with the hBN filler. The microstructure seen on the surface has many defects in coating layers such as spalling and blisters, but overall the coating surface still looks smooth.

Fig. 1, *b* shows the microstructure of ZS2 thermal shock samples with a combination of zircon sand with MoS_2 filler showing the surface morphology of the coating delaminates onto the substrate. Fig. 1, *c* shows the microstructure of the ZS3 thermal shock sample, which is a zircon sand coating combined with graphite filler. From the morphology, it can be seen that some of the coating still survives but there are some areas that are peeled off to the substrate. Fig. 1, *d* shows

the microstructure of the ZS4 thermal shock sample, which is a variation of zircon sand coating with hybrid fillers hBN, MoS_2, and graphite. From the microstructure image, it can be seen that the coating surface looks homogeneous even though there are several small holes.

Table 3 presents the EDS data of the zircon sand coating with various fillers after thermal shock treatment. The ZS1 EDS results of elements measured on the coating surface area show that boron dominates in its distribution more than zircon. The ZS2 EDS data shows that the Fe content of the steel substrate dominates on the sample surface due to delamination. From the ZS3 EDS data, it is shown that the coating surface that still survives is dominated by zircon content, while graphite does not exist in the coating surface area.

Meanwhile, the ZS4 EDS data shows that the elements forming of the matrix and filler coating are evenly distributed in the coating surface area.

Table 3

EDS data results of zircon sand based composite ceramic coating after thermal shock treatment

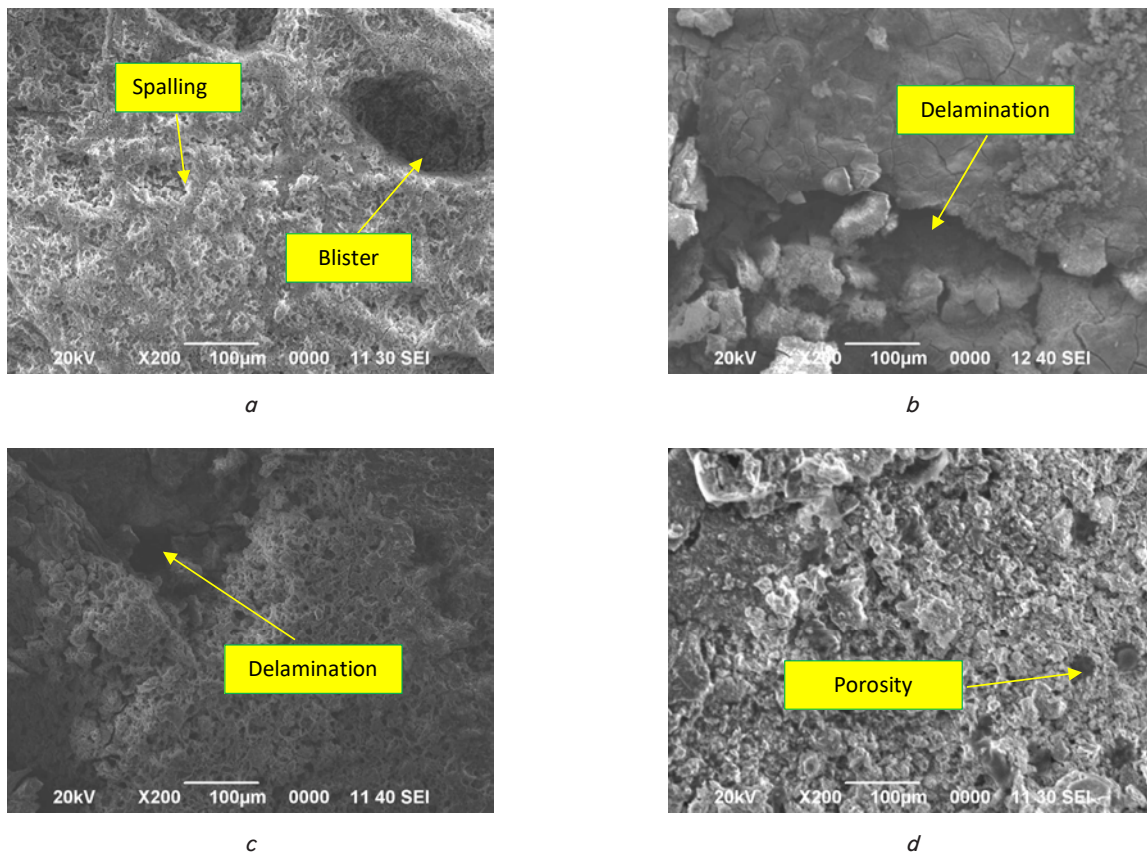| Sample Code	Element (wt %)									
	C	O	Na	Si	S	Cl	Fe	Zr	B	Mo
ZS1	–	37.11	1.46	38.42	–	–	2.64	1.01	19.35	–
ZS2	–	19.09	–	–	–	–	79.02	–	–	1.89
ZS3	–	30.36	7.50	24.42	–	0.73	28.63	8.37		–
ZS4	18.36	37.25	8.67	26.08	1.12	0.74	5.68	0.61	–	1.50

a

b

c

d

Fig. 1. Microstructure of zircon sand based composite ceramic coating after thermal shock treatment:
a – ZS1; *b* – ZS2; *c* – ZS3; *d* – ZS4

5. 2. 2. Purified zircon based ceramic composite coating

Fig. 2, *a–d* shows the surface microstructure of purified zircon coating samples with various fillers used, which are treated with thermal shock at 600 °C for 10 minutes and then quenched.

Fig. 2, *a* represents the microstructure of the ZP1 thermal shock sample where purified zircon is combined with the hBN filler. The microstructure shows a homogeneous coating surface even though there are some defects such as porosity and peeling. Fig. 2, *b* shows the microstructure of ZP2 thermal shock samples with a combination of purified zircon with the MoS_2 filler. The coating surface looks homogeneous although there is delamination and porosity. Fig. 2, *c* shows the microstructure of the ZP3 thermal shock sample, which is a purified zircon coating combined with the graphite filler. From the microstructure of the coating surface, it can be seen that there are several areas that have peeled off to the substrate or delamination. Fig. 2, *d* shows the microstructure of the ZP4 thermal shock sample, which is a purified zircon coating combined with the hybrid filler. From the microstructure of the coating surface, it can be seen that the coating has an even distribution even though there are some defects such as cracks.

Table 4 gives the EDS data of the purified zircon based coating with various fillers after thermal shock treatment. The ZP1 EDS results show that the coating content on the surface is dominated by zircon.

The ZP2 EDS results show that the matrix and filler coating element content tends to be evenly distributed. From the ZP3 EDS data, it is seen that there is no zirconia and graphite content, which indicates a lack of strength of the coating during the thermal shock process. And the ZP4 EDS data also shows that the coating element content is fairly even, indicating that the coating held up well during the thermal shock test.

Table 4

EDS data results of purified zircon based composite ceramic coating after thermal shock treatment

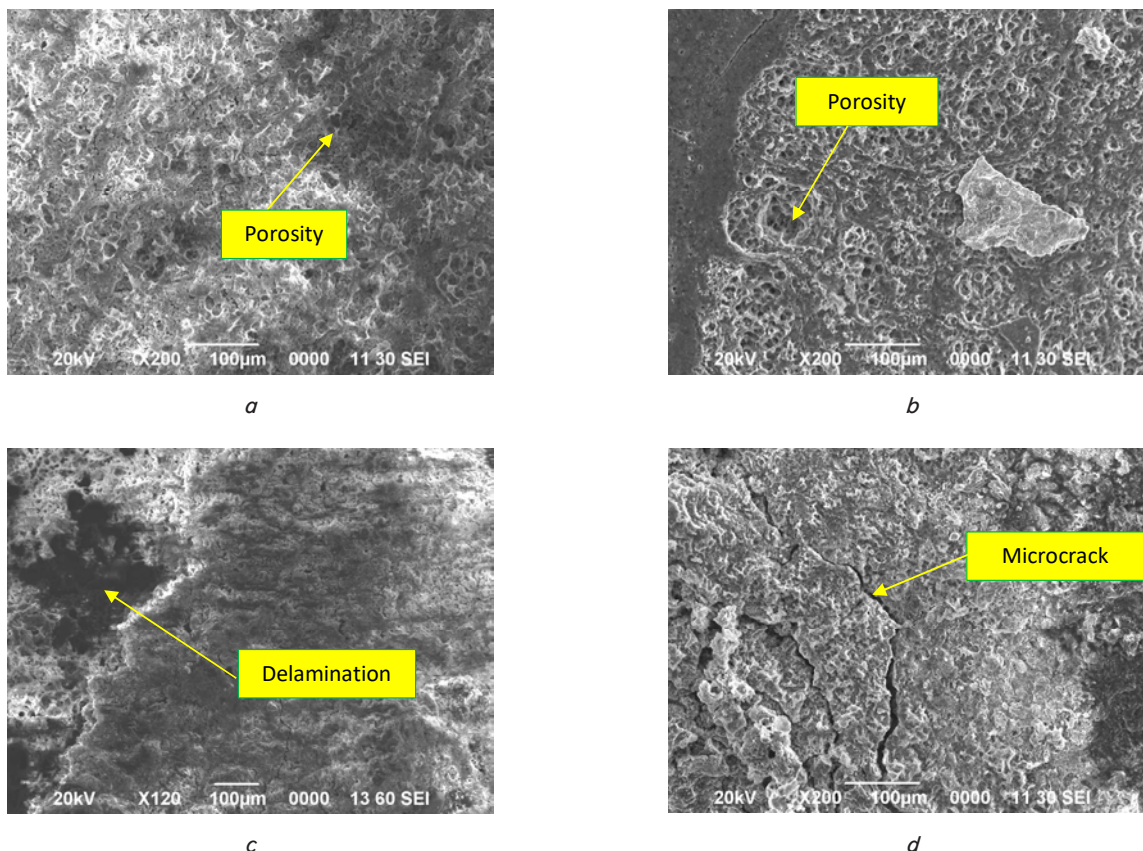| Sample Code	Element (wt %)									
	C	O	Na	Si	S	Cl	Fe	Zr	B	Mo
ZP1	–	43.48	2.30	41.94	–	–	3.15	9.13	–	–
ZP2	–	–	–	70.56	6.46	–	8.12	8.98	–	5.88
ZP3	–	30.26	–	30.26	–	0.48	39.00	–	–	–
ZP4	–	37.97	5.34	39.88	0.46	–	13.43	1.35	–	1.57

a

b

c

d

Fig. 2. Microstructure of purified zircon based composite ceramic coating after thermal shock treatment:
a — ZP1; *b* — ZP2; *c* — ZP3; *d* — ZP4

5. 3. Fouling resistance

5. 3. 1. Zircon sand based ceramic composite coating

Fig. 3, *a–d* show the microstructure of the zircon sand coating with various fillers that were polished with sodium sulfate powder (Na_2SO_4), then heated in a muffle furnace at 600 °C for 24 hours and cooled at room temperature. Fig. 3, *a* shows the ZS1 sample result of fouling resistance where the coating is still visible but slightly delaminated. Fig. 3, *b* shows the microstructure of the ZS2 fouling resistance sample, where the microstructure image shows the amount of Na_2SO_4 attached to the coating surface. Whereas Fig. 3, *c* shows the microstructure of the ZS3 fouling resistance sample, where the microstructure image shows that most of the coating surface is still filled with attached Na_2SO_4. Fig. 3, *d* shows the microstructure of the ZS4 sample of fouling resistance, which is a variation of zircon sand coating with hybrid fillers hBN, MoS_2, and graphite. It can be seen from the microstructure that Na_2SO_4 on the surface of the coating is partially lifted and there is a small part left behind.

Table 5 presents the EDS data of the zircon sand coating with various fillers after fouling treatment. From the EDS data of the ZS1 sample, it can be seen that the Na_2SO_4 content on the surface of the coating is very small, which indicates that the Na_2SO_4 powder does not stick much.

The EDS data of the ZS2 and ZS3 samples showed quite high levels of Na_2SO_4 on the surface of the coating indicating a lack of fouling resistance of the coating. Meanwhile, the EDS data of the ZS4 sample showed that the Na_2SO_4 content on the surface of the coating was close to that of ZS1, so that the fouling resistance of this hybrid filler was almost the same as that of hBN.

The fouling test using Na_2SO_4 powder attached to the coating surface will cause friction, which results in defects. So it is very necessary to see and compare the defects that arise after the anti-fouling test. Fig. 4 presents an analysis image of the defect coating surface after the fouling test using ImageJ software.

Table 5

EDS data results of zircon sand based composite ceramic coating after fouling treatment

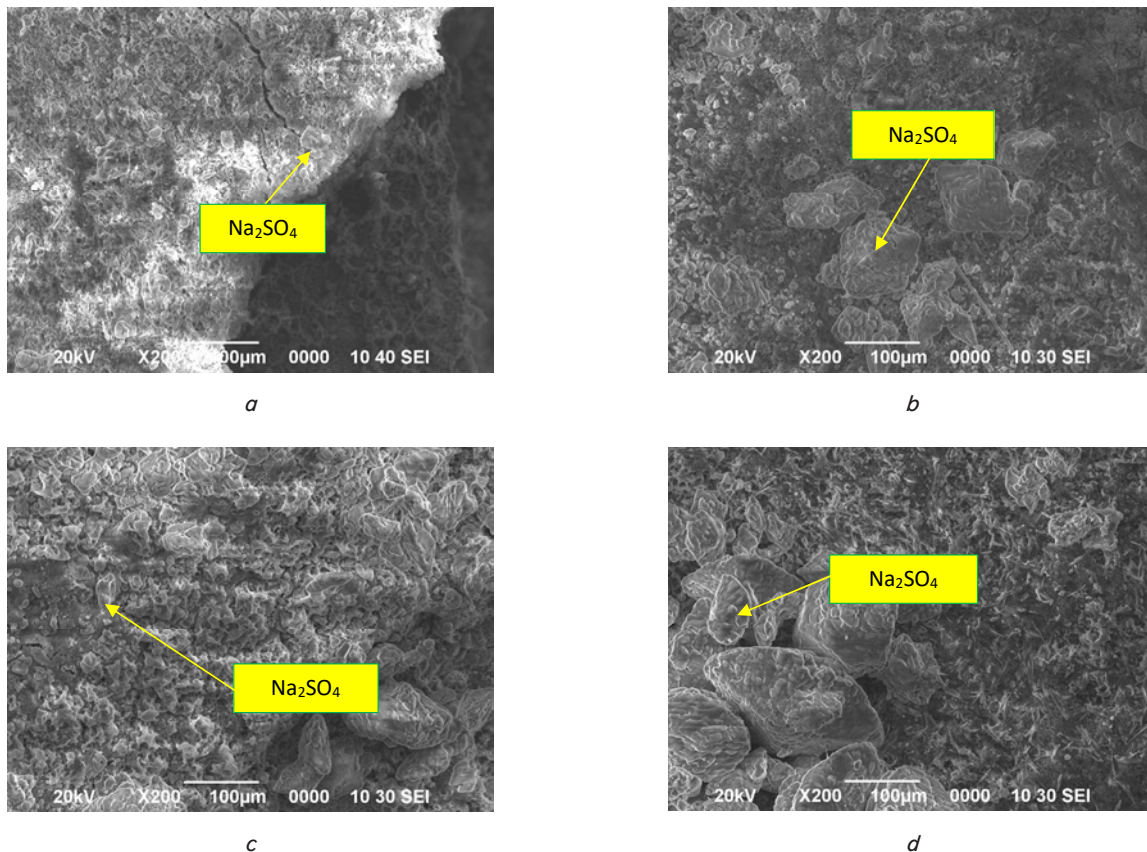| Sample Code	Element (wt %)									
	C	O	Na	S	Si	Cl	Fe	Zr	B	Mo
ZS1	–	35.05	5.89	3.76	33.70	0.82	20.80	–	–	–
ZS2	–	39.91	12.40	10.53	32.62	–	4.54	–	–	–
ZS3	–	37.51	19.59	16.18	17.07	–	9.65	–	–	–
ZS4	–	35.15	6.70	7.31	26.79	1.26	15.28	7.51	–	–

Fig. 3. Microstructure of zircon sand based composite ceramic coating after fouling treatment:
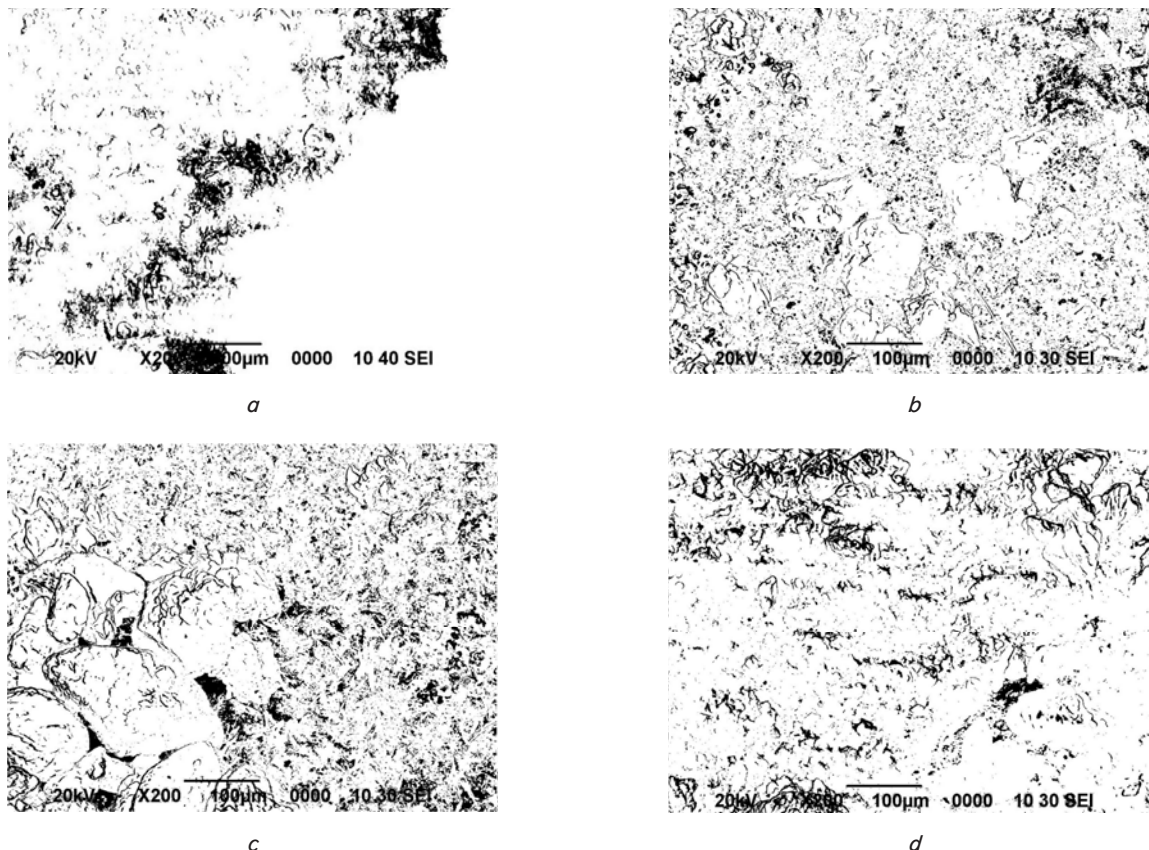*a* – ZS1; *b* – ZS2; *c* – ZS3; *d* – ZS4

Fig. 4. Image profile of zircon sand based coating surface defects after fouling test using ImageJ Software: *a* — ZS1; *b* — ZS2; *c* — ZS3; *d* — ZS4

Defects are in the form of porosity, crack, delamination and blister. Fig. 4, *a* shows the surface defect profile with less area as well as Fig. 4, *d*. Fig. 4, *b*, *c* shows the larger surface defects of the coating. ImageJ software calculates the stacks that occur on the surface of the coating. From these stacks profiles, particles can then be analyzed to obtain the percentage of porosity as shown in Fig. 5. From Fig. 5, it can be seen that the percentage porosity of ZS1 and ZS4 is lower than that of ZS2 and ZS3.
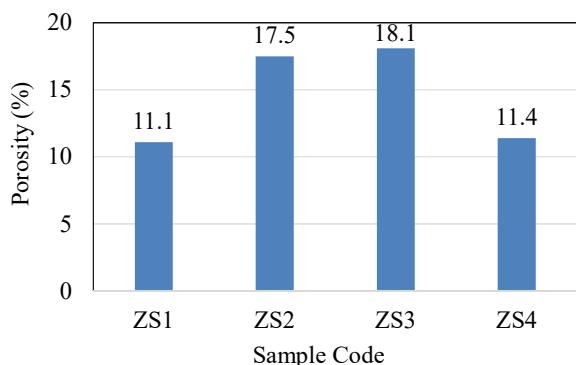

Fig. 5. Porosity percentage of zircon sand based coating with Various Fillers after Fouling Test

5. 3. 2. Purified zircon based ceramic composite coating

Fig. 6, *a–d* shows the microstructure of the purified zircon coating with various fillers that were polished with sodium sulfate powder (Na_2SO_4), then heated in a muffle furnace at 600 °C for 24 hours and cooled at room temperature. Fig. 6, *a* shows the result of the ZP1 sample of the fouling resistance test, where the microstructure image shows that

the surface of the coating is filled with Na_2SO_4 powder and a lot of the coating is peeled off. Meanwhile, Fig. 6, *b* shows the microstructure of the ZP2 fouling resistance sample. The surface of the coating is filled with Na_2SO_4 powder, which is still retained and a small part is peeled off.

Fig. 6, *c* shows the microstructure of the ZP3 fouling resistance sample. After the anti-fouling test, the microstructure of the sample showed that Na_2SO_4 powder grains filled the surface of the coating and some of the coating was peeled off. Fig. 6, *d* shows the microstructure of the ZP4 fouling resistance test sample. From the results of the microstructure, it is shown that there are not many Na_2SO_4 grains attached to the coating even though they are still present in some areas. Table 6 gives the EDS data of purified zircon based coating with various fillers after fouling treatment.

From Table 6, it can be seen that the Na_2SO_4 content on the coating surface of the ZP1 sample is the highest compared to ZP2, ZP3 and ZP4. ZP4, which uses the hybrid filler and the purified zircon matrix has the best fouling resistance because it has the least amount of Na_2SO_4 on the coating surface.

Fig. 7, *a* shows surface defects in the form of uniform cracks and small porosity. In Fig. 7, *b*, there are many localized porosity and cracks. Fig. 7, *c* shows the porosity and delamination on the coating surface, as similarly shown in Fig. 7, *d*, there is some localized porosity and delamination. From the results of surface particle analysis using ImageJ Software, the results of calculating the surface porosity percentage of the coating are shown in Fig. 8. From Fig. 8, it can be seen that the coating with the hybrid filler has the lowest percentage of porosity compared to other fillers, but the value is not significantly different.
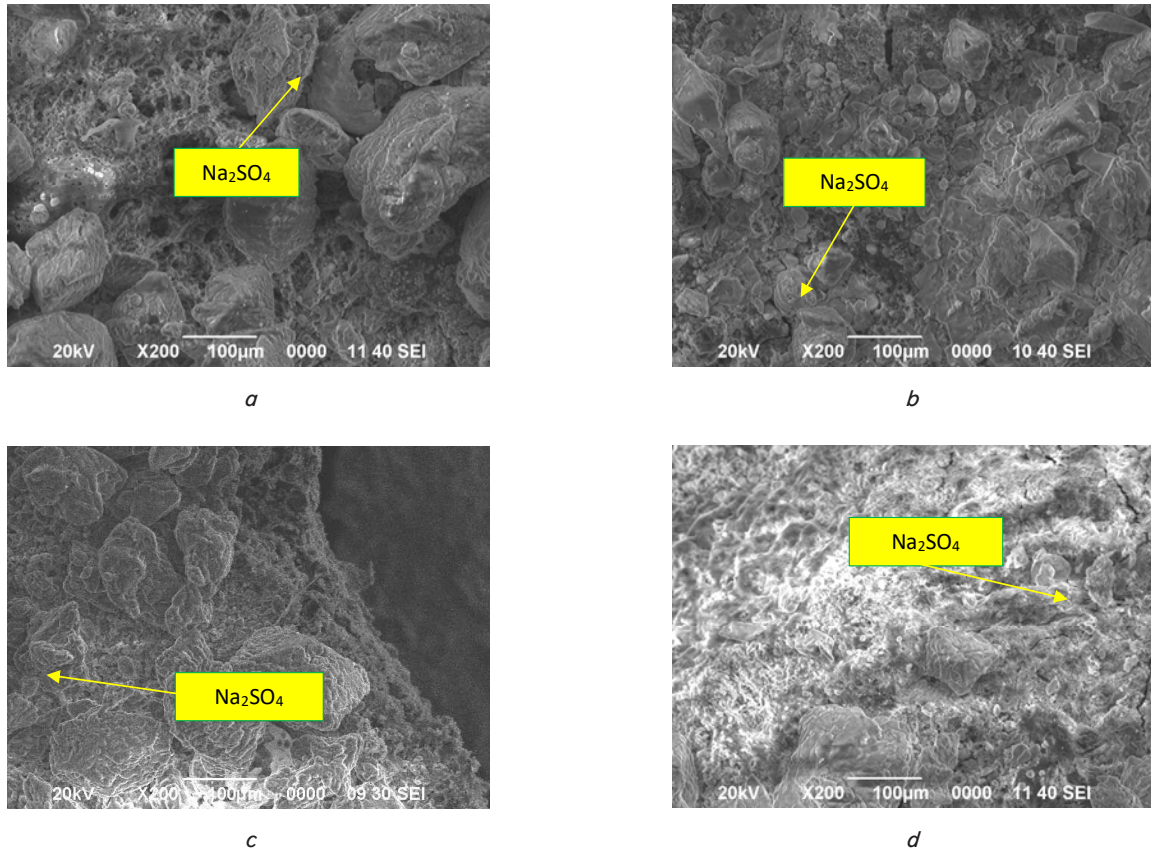
Fig. 6. Microstructure of purified zircon based composite ceramic coating after fouling treatment:
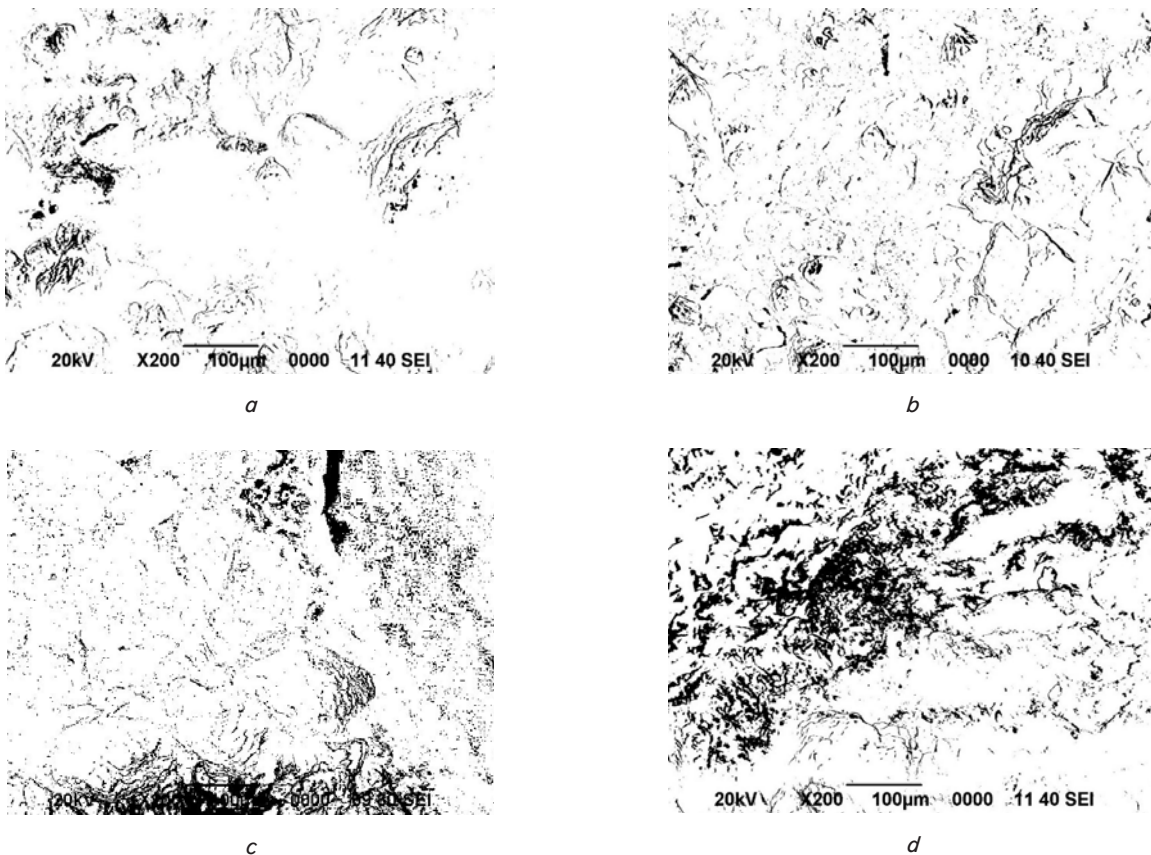a − ZP1; b − ZP2; c − ZP3; d − ZP4

Fig. 7. Image profile of coating surface defects after fouling test using ImageJ Software: a − ZP1; b − ZP2; c − ZP3; d − ZP4

EDS data results of purified zircon based composite ceramic coating after fouling treatment

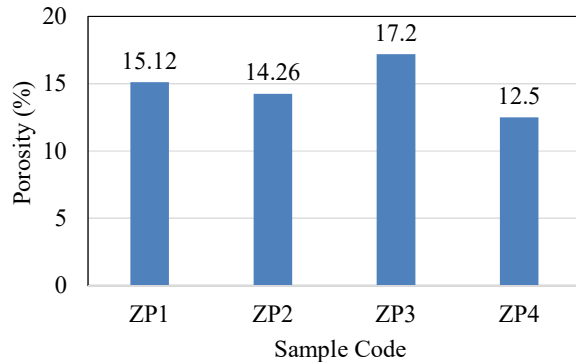| Sample Code	Element (wt %)									
	C	O	Na	S	Si	Cl	Fe	Zr	B	Mo
ZP1	–	23.09	23.04	14.00	1.34	–	38.54	–	–	–
ZP2	–	35.10	14.81	12.45	24.55	2.34	10.75	–	–	–
ZP3	–	34.25	11.93	9.69	25.61	0.76	17.76	–	–	–
ZP4	–	40.20	10.17	7.67	32.10	–	9.86	–	–	–

Fig. 8. Porosity percentage of purified zircon based coating with various fillers after fouling test

6. Discussion of the research results of thermal shock and fouling resistance

XRF analysis aims to see changes in the content of zirconia and other elements such as silica, titania, alumina, and other elements contained in zircon sand. From Table 2, which is the result of the XRF test for the oxide content of zircon sand and purified zircon, it can be seen that the zircon content of purified zircon is increased compared to zircon sand. This was followed by a decrease in the silica content of the purified zircon. Titania is also reduced because the acid solvent used can dissolve titania, titania will dissolve in heated high concentrations of HCl [37]. Increasing the zirconia content is very important to increase the thermal stability so that when it is used as a raw material for coatings, it can produce high-temperature resistant coatings. Zirconium occurs in nature not as a free element, but in the form of zirconium silicate in zircon sand, zirconium oxide in baddeleyite, zirconium carbonate with sodium, calcium, and so on. Zirconium is also found as an impurity in some of the minerals titanate, niobanate, tantaloniobanate and so on. Beddeleyite and zircon are widely used because they have more value in the industrial world. All Zr ores contain about 1–3 % hafnium. Chemically, Zr and Hf have very similar properties so that they cannot be separated by a common reduction process, however, nuclear properties are very much different [38]. In order to increase the purity of the zirconia content, in the future it is possible to vary the calcination temperature and the ratio of the composition of zircon sand to the alkali in the alkali fusion process in order to obtain more optimum results.

The results of the thermal shock and anti-fouling resistance coating tests were analyzed from the microstructure and EDS content. This is done to determine the damage and defects that arise after the thermal shock and anti-fouling processes and changes in the elemental content of the coating. Fig. 1, 2 show the images of the microstructure results of the thermal shock test, which showed that almost all variations have delamination on the coating surface. This is due to a difference in thermal expansion between the coating and the steel substrate [39]. Thermal shock testing at high temperatures produces surface tension. When the applied thermal stress exceeds the resistance stress, this will cause defects on the coating surface. The most common defects are creeping cracks and small pores [40]. The microstructure of the coating with purified zircon has a finer grain size and more homogeneous surface coating because the results of purified zircon have a finer powder texture than zircon sand, so when applied as a coating, the mixture becomes perfectly blended. The resistance of coatings with various fillers, for hBN and hybrid fillers, has a microstructure that has minimal defects, while the coating with graphite peels off the most. The results of the anti-fouling test from Fig. 3 and Fig. 6 also showed the same phenomenon, the coating with the MoS_2 and graphite filler had fouling on the surface. This is because the coating is easily peeled off to the substrate, and there will be a reaction between the sodium and sulfide salts with the metal [41]. One solution to overcome in the future is to add a bond coat, which has an intermediate thermal expansion between the coating and the substrate to reduce the occurrence of cracks.

The coating with purified zircon has better thermal shock resistance compared to the coating with zircon sand, as seen from the results of the microstructure, which has minimal defects and good coating adhesion characterized by an average delamination of less than 1/3 area compared to zircon sand coatings. Residual thermal stresses are generated when there is an impact on the sample when it is heated and then rapidly cooled (quenched). Due to the weak interface structure, the crack will propagate on the interface. The cracks and porosity that are formed are a way for the coating to release the stresses that occur and can result in spalling on the surface of the ceramic coating [42]. The EDS results in Tables 3, 4 do not contain too many substrate elements. For fouling resistance results, the difference between the coatings is not too significant. From Tables 5, 6, it can be seen that the coating surface after the fouling test contained Na and S. The results of the antifouling test showed that the coating with hBN, MoS_2 and graphite contained fouling on the coating surface. This is because the coating is easily peeled off on the substrate, and a reaction will occur between the sodium and sulfide salts with the metal [41]. From the percentage of porosity in Fig. 5 and Fig. 8, it is also shown that the coating with purified zircon produces fewer pores, although it is not significant. For the variety purified zircon and zircon sand of fillers used, the resistance to thermal shock and fouling can be seen, for hBN and hybrid fillers, the results are better in terms of microstructure and porosity in Fig. 4 and Fig. 7, which tends to be slightly deformed, does not peel off easily, and clean areas of sodium sulfate after the anti-fouling test. By using the hybrid filler in coatings, it is

possible to reduce the use of hBN, which will greatly affect the economic side, which can reduce costs.

porosity, which was around 11 %. This shows that hybrid filler can be used as an alternative for filler coating to reduce costs.

7. Conclusions

1. The refining process of Kalimantan zircon sand shows an increase in zirconia content from 59 % to 68 %. This is because some of the SiO_2 quartz bonds are detached from ZrO_2. This shows that the purified ZrO_2 is suitable for further use as a coating material.

2. For thermal shock resistance, the coating with purified zircon has better thermal shock results compared to the coating with zircon sand, as seen from the microstructure, which has minimal defects and good adhesion, and the EDS results do not contain too many substrate elements (Fe). Meanwhile, for the variation of filler used, hBN and hybrid filler have fewer defects after thermal shock treatment and better adhesion because not much coating is peeled off.

3. For the fouling resistance of the coating with the variation of the zircon matrix used, the increase in zircon content from 59 % to 68 % showed results that were not significantly different. In several coating studies using ZrO_2, pure ZrO_2 powder is usually used with a ZrO_2 content above 90 %. So it is necessary to develop a zircon purification process in order to obtain higher levels of ZrO_2. Meanwhile, for the variation of filler used, the hybrid filler showed the lowest percentage of

Conflict of interest

The authors declare that they have no conflict of interest in relation to this research, whether financial, personal, authorship or otherwise, that could affect the research and its results presented in this paper.

Data availability

The manuscript has no associated data.

References

1. Ahmed, G. M. S., Mohiuddin, Mohd. V., Sultana, S., Dora, H. K., Singh, V. D. (2015). Microstructure Analysis and Evaluation of Mechanical Properties of Nickel Based Super Alloy CCA617. Materials Today: Proceedings, 2 (4-5), 1260–1269. doi: https://doi.org/10.1016/j.matpr.2015.07.041

2. Mabruri, E., Syahlan, Z. A., Sahlan, Prifiharni, S., Anwar, M. S., Chandra, S. A. et al. (2017). Influence of Austenitizing Heat Treatment on the Properties of the Tempered Type 410-1Mo Stainless Steel. IOP Conference Series: Materials Science and Engineering, 202, 012085. doi: https://doi.org/10.1088/1757-899x/202/1/012085

3. Müller-Steinhagen, H., Malayeri, M. R., Watkinson, A. P. (2011). Heat Exchanger Fouling: Mitigation and Cleaning Strategies. Heat Transfer Engineering, 32 (3-4), 189–196. doi: https://doi.org/10.1080/01457632.2010.503108

4. Gomes da Cruz, L., Ishiyama, E. M., Boxler, C., Augustin, W., Scholl, S., Wilson, D. I. (2015). Value pricing of surface coatings for mitigating heat exchanger fouling. Food and Bioproducts Processing, 93, 343–363. doi: https://doi.org/10.1016/j.fbp.2014.05.003

5. Santos, O., Anehamre, J., Wictor, C., Tornqvist, A., Nilsson, M. (2013). Minimizing crude oil fouling by modifying the surface of heat exchangers with a flexible ceramic coating. In Proc. Heat Exchanger Fouling & Cleaning X, 79–84.

6. Wang, J., Yuan, Y., Chi, Z., Zhang, G. (2018). Development and application of anti-fouling ceramic coating for high-sodium coal-fired boilers. Journal of the Energy Institute, 91 (6), 962–969. doi: https://doi.org/10.1016/j.joei.2017.08.003

7. Zhang, Z., Chen, H., Wang, Y., Wang, G., Li, L., Zhong, M., Bai, H. (2022). Effect of sodium silicate binder on the performance of ceramic coatings on copper prepared by the slurry method. Surface and Coatings Technology, 448, 128868. doi: https://doi.org/10.1016/j.surfcoat.2022.128868

8. Hirvonen, A., Nowak, R., Yamamoto, Y., Sekino, T., Niihara, K. (2006). Fabrication, structure, mechanical and thermal properties of zirconia-based ceramic nanocomposites. Journal of the European Ceramic Society, 26 (8), 1497–1505. doi: https://doi.org/10.1016/j.jeurceramsoc.2005.03.232

9. Fazel, M., Jazi, M. R. G., Bahramzadeh, S., Bakhshi, S. R., Ramazani, M. (2014). Effect of solid lubricant particles on room and elevated temperature tribological properties of Ni–SiC composite coating. Surface and Coatings Technology, 254, 252–259. doi: https://doi.org/10.1016/j.surfcoat.2014.06.027

10. Kumar, R., Antonov, M. (2021). Self-lubricating materials for extreme temperature tribo-applications. Materials Today: Proceedings, 44, 4583–4589. doi: https://doi.org/10.1016/j.matpr.2020.10.824

11. Sun, X., Zhang, J., Pan, W., Wang, W., Tang, C. (2023). A review on the preparation and application of BN composite coatings. Ceramics International, 49 (1), 24–39. doi: https://doi.org/10.1016/j.ceramint.2022.10.259

12. Mischke, P. (2014). Film Formation: in Modern Paint Systems. Hannover, Germany: Vincentz Network. doi: https://doi.org/10.1515/9783748602262

13. Wu, Z., Li, S., Zhang, P., Wang, C., Deng, C., Mao, J., Li, W., Tu, X. (2022). Controllable in-situ synthesis of MoS_2/C in plasma-sprayed YSZ coatings: Microstructure, mechanical and tribological properties. Surface and Coatings Technology, 448, 128895. doi: https://doi.org/10.1016/j.surfcoat.2022.128895

14. Tuo, Y., Yang, Z., Guo, Z., Chen, Y., Hao, J., Zhao, Q. et al. (2023). Pore structure optimization of MoS_2/Al_2O_3 self-lubricating ceramic coating for improving corrosion resistance. Vacuum, 207, 111687. doi: https://doi.org/10.1016/j.vacuum.2022.111687

15. Marcinauskas, L., Mathew, J. S., Milieška, M., Aikas, M., Kalin, M. (2023). Influence of graphite content on the tribological properties of plasma sprayed alumina-graphite coatings. Surfaces and Interfaces, 38, 102763. doi: https://doi.org/10.1016/j.surfin.2023.102763

16. Eichler, J., Lesniak, C. (2008). Boron nitride (BN) and BN composites for high-temperature applications. Journal of the European Ceramic Society, 28 (5), 1105–1109. doi: https://doi.org/10.1016/j.jeurceramsoc.2007.09.005

17. Zhao, W., Pan, J., Fang, Y., Che, X., Wang, D., Bu, K., Huang, F. (2018). Metastable MoS_2: Crystal Structure, Electronic Band Structure, Synthetic Approach and Intriguing Physical Properties. Chemistry - A European Journal, 24 (60), 15942–15954. doi: https://doi.org/10.1002/chem.201801018

18. Jara, A. D., Betemariam, A., Woldetinsae, G., Kim, J. Y. (2019). Purification, application and current market trend of natural graphite: A review. International Journal of Mining Science and Technology, 29 (5), 671–689. doi: https://doi.org/10.1016/j.ijmst.2019.04.003

19. Lee, K. N., Waters, D. L., Puleo, B. J., Garg, A., Jennings, W. D., Costa, G., Sacksteder, D. E. (2020). Development of oxide-based High temperature environmental barrier coatings for ceramic matrix composites via the slurry process. Journal of the European Ceramic Society, 41 (2), 1639–1653. doi: https://doi.org/10.1016/j.jeurceramsoc.2020.10.012

20. Wang, J., Yuan, Y., Chi, Z., Zhang, G. (2018). High-temperature sulfur corrosion behavior of h-BN-based ceramic coating prepared by slurry method. Materials Chemistry and Physics, 206, 186–192. doi: https://doi.org/10.1016/j.matchemphys.2017.12.025

21. Jiapei, J., Yongnan, C., Chaoping, J., Yong, Z., Qinyang, Z., Zhen, Z. et al. (2022). Composite ceramic coating with enhanced thermal shock resistance formed by the in-situ synthesis of nano-ZrO_2. Ceramics International, 48 (8), 10629–10637. doi: https://doi.org/10.1016/j.ceramint.2021.12.277

22. Liu, Q., Hu, X. P., Zhu, W., Liu, G. L., Guo, J. W., Bin, J. (2022). Thermal shock performance and failure behavior of $Zr_6Ta_2O_{17}$-8YSZ double-ceramic-layer thermal barrier coatings prepared by atmospheric plasma spraying. Ceramics International, 48 (17), 24402–24410. doi: https://doi.org/10.1016/j.ceramint.2022.05.046

23. Sigaroodi, M. R. J., Poursaeidi, E., Rahimi, J., Jamalabad, Y. Y. (2023). Heat treatment effect on coating shock resistance of thermal barrier coating system with different types of bond coat. Journal of the European Ceramic Society, 43 (8), 3658–3675. doi: https://doi.org/10.1016/j.jeurceramsoc.2023.01.035

24. Cañas, E., Rosado, E., Alcázar, C., Orts, M. J., Moreno, R., Sánchez, E. (2022). Challenging zircon coatings by suspension plasma spraying. Journal of the European Ceramic Society, 42 (10), 4369–4376. doi: https://doi.org/10.1016/j.jeurceramsoc.2022.03.049

25. Barish, J. A., Goddard, J. M. (2013). Anti-fouling surface modified stainless steel for food processing. Food and Bioproducts Processing, 91 (4), 352–361. doi: https://doi.org/10.1016/j.fbp.2013.01.003

26. Ishiyama, E. M., Paterson, W. R., Wilson, D. I. (2008). Thermo-hydraulic channelling in parallel heat exchangers subject to fouling. Chemical Engineering Science, 63 (13), 3400–3410. doi: https://doi.org/10.1016/j.ces.2008.04.008

27. Ayala, L. (2015). Technical handbook on zirconium and zirconium compounds. Zircon Industry Association.

28. Musyarofah, Lestari, N. D., Nurlaila, R., Muwwaqor, N. F., Triwikantoro, Pratapa, S. (2019). Synthesis of high-purity zircon, zirconia, and silica nanopowders from local zircon sand. Ceramics International, 45 (6), 6639–6647. doi: https://doi.org/10.1016/j.ceramint.2018.12.152

29. Yuhelda, Y., Amalia, D., Nugraha, E. P. (2017). Processing zirconia through zircon sand smelting with NaOH as a flux. Indonesian Mining Journal, 19 (1), 39–49. doi: https://doi.org/10.30556/imj.vol19.no1.2016.364

30. Yamagata, C., Andrade, J. B., Ussui, V., de Lima, N. B., Paschoal, J. O. A. (2008). High Purity Zirconia and Silica Powders via Wet Process: Alkali Fusion of Zircon Sand. Materials Science Forum, 591-593, 771–776. doi: https://doi.org/10.4028/www.scientific.net/msf.591-593.771

31. Ray, H. S., Ghosh, A. (2010). Principles of Extractive Metallurgy. New Delhi: New Age International (P) Limites Publisher.

32. Mutimmah, Yuswono, S., Akbar, D. W., Nugroho, T. P., Rahman, Nofrizal, R., Ikono, Siswanto, Rochman, N. T. (2013). Optimization of Zirconia Extraction Made from Silicate Zircon Sand Through Base Reduction. Proceedings of Semirata FMIPA, University of Lampung, 401–404.

33. Sarkar, M., Mandal, N. (2022). Solid lubricant materials for high temperature application: A review. Materials Today: Proceedings, 66, 3762–3768. doi: https://doi.org/10.1016/j.matpr.2022.06.030

34. Bittmann, B., Haupert, F., Schlarb, A. K. (2009). Ultrasonic dispersion of inorganic nanoparticles in epoxy resin. Ultrasonics Sonochemistry, 16 (5), 622–628. doi: https://doi.org/10.1016/j.ultsonch.2009.01.006

35. Billotte, C., Fotsing, E. R., Ruiz, E. (2017). Optimization of Alumina Slurry for Oxide-Oxide Ceramic Composites Manufactured by Injection Molding. Advances in Materials Science and Engineering, 2017, 1–9. doi: https://doi.org/10.1155/2017/2748070

36. Tajima, R., Kato, Y. (2011). Comparison of threshold algorithms for automatic image processing of rice roots using freeware ImageJ. Field Crops Research, 121 (3), 460–463. doi: https://doi.org/10.1016/j.fcr.2011.01.015

37. Nguyen, M., Bang, J., Kim, Y., Bin, A., Hwang, K., Pham, V.-H., Kwon, W.-T. (2018). Anti-Fouling Ceramic Coating for Improving the Energy Efficiency of Steel Boiler Systems. Coatings, 8 (10), 353. https://doi.org/10.3390/coatings8100353

38. Poernomo, H. (2012). Zirconium General Information. Yogyakarta: National Nuclear Energy Agency, Center for Material Process and Accelerator Technology.

39. Donachie, M. (2000). Titanium: A Technical Guide. ASM International. doi: https://doi.org/10.31399/asm.tb.ttg2.9781627082693

40. Xiao, K., Xue, W., Li, Z., Wang, J., Li, X., Dong, C. et al. (2018). Effect of sintering temperature on the microstructure and performance of a ceramic coating obtained by the slurry method. Ceramics International, 44 (10), 11180–11186. doi: https://doi.org/10.1016/j.ceramint.2018.03.147

41. Lee, S.-H., Themelis, N. J., Castaldi, M. J. (2007). High-Temperature Corrosion in Waste-to-Energy Boilers. Journal of Thermal Spray Technology, 16 (1), 104–110. doi: https://doi.org/10.1007/s11666-006-9005-4

42. Cheng, Y., Miu, L., Hou, B. (1990). Fatigue Strength[M]. Beijing: China Railway Press, 11.